

## On the morphology of SrCO<sub>3</sub> crystals grown at the interface between two immiscible liquids

SATYANARAYANA REDDY, DEBABRATA RAUTARAY, S R SAINKAR and MURALI SASTRY\*

Materials Chemistry Division, National Chemical Laboratory, Pune 411 008, India

MS received 21 August 2002

**Abstract.** In this paper we report on the growth of strontianite crystals at the interface between an aqueous solution of Sr<sup>2+</sup> ions and organic solutions of chloroform and hexane containing fatty acid/fatty amine molecules by reaction with sodium carbonate. When fatty acid was used as an additive at the interface, the crystals grown were self-assembled needle shaped strontianite crystallites branching out from the seed crystal via secondary nucleation. Under identical conditions of supersaturation, the presence of fatty amine molecules at the liquid–liquid interface resulted in needle shaped strontianite crystals with spherical crystallites arranged around central needles. This clearly indicates that the functionality of the head group of the amphiphiles at the liquid–liquid interface affects the morphology of the strontium carbonate crystals formed. The use of interfacial effects such as dielectric discontinuity, polarity and finite solubility of the two solvents etc opens up exciting possibilities for tailoring the morphology of crystals at the liquid–liquid interface and is currently not possible in the more popular crystal growth with similar amphiphiles at the air–water interface.

**Keywords.** Crystal morphology; interfaces; minerals; solvents; polycrystalline deposition.

### 1. Introduction

Development of strategies to grow crystals of controllable structure, size, morphology and superstructures of pre-defined organizational order is an important goal in crystal engineering with tremendous implications in the ceramic industry (Heuer *et al* 1992; Bunker *et al* 1994). Lured by the exquisite control that biological organisms exert over mineral nucleation and growth (both amorphous and crystalline) by a process known as biomineralization (Mann *et al* 1989; Addadi and Weiner 1992; Mann 1993, 1996, 1997; Weiner and Addadi 1997; McGrath 2001), materials scientists are attempting to develop biomimetic approaches for the synthesis of advanced ceramic materials. It is now established that an important requirement for biomineralization is epitaxy between the crystal nucleating face and underlying bio-organic surface and consequently, biomimetic surfaces such as those presented by Langmuir monolayers (Heywood and Mann 1992a,b, 1994; Litvin *et al* 1997; Buijnsters 2001), self-assembled monolayers (SAMs) on planar (Kuther *et al* 1998a; Aizenberg *et al* 1999) and nanoscale curved surfaces (Nagtegaal *et al* 1998; Kuther *et al* 1998b,c, 1999) as well as functionalized polymer surfaces (Falini *et al* 1994; Feng and Bein 1994) have been studied in great detail. Attempts have also been made to control the morphology of crystals by addition of

suitable crystallization inhibitors (Bromley *et al* 1993; Qi *et al* 2000; Uchida *et al* 2001) and carrying out crystal growth in constrained environments such as those afforded by microemulsions (Hopwood and Mann 1997; Li and Mann 2000).

While it is clear from the above that a number of templating interfaces both biological and biomimetic have been used in the growth of crystals, there is very little work on crystal growth at the liquid–liquid interface using suitably immobilized templating molecules at the interface. The liquid–liquid interface is an important area of research in chemistry that impacts understanding of the stability of emulsions, chemical separation processes, interfacial catalysis as well as many processes in biological systems (Bowers *et al* 2001). Only recently has the liquid–liquid interface been viewed seriously as a medium for the organization of micron sized objects (Bowen *et al* 2001) and growth of nanoparticles of CdS (Sathaye *et al* 2000). Following our recent work on the use of lipid bilayer stacks in the growth of SrCO<sub>3</sub> crystals (Sastry *et al* 2001) and our preliminary report on the growth of BaSO<sub>4</sub> crystals at the liquid–liquid interface (Ray *et al* 2001), we present herein details of our investigation into the growth of SrCO<sub>3</sub> (strontianite) crystals at the interface between an aqueous solution of Sr<sup>2+</sup> ions and organic solutions of chloroform and hexane containing fatty acid/fatty amine molecules by reaction with sodium carbonate. The process is seemingly similar to crystallization at the air–water interface with anionic Langmuir monolayers as the template with the following important differences. The

\*Author for correspondence

magnitude of the dielectric discontinuity between water–organic solution and water–air would be different and could lead to important differences in the electrostatics of complexation of the  $\text{Sr}^{2+}$  ions with the surfactant molecules at the interface. Furthermore, the finite solubility of the two solutions would lead to a region of the interface with a much broader gradation in the dielectric function that could in turn influence the electrostatics of the metal ion complexation with the lipid molecules as well as the organization of the templating lipid molecules in the interfacial region. The solvation of the hydrocarbon chains in the organic phase would also contribute to disruption in the ordering of the surfactant molecules at the water–organic solution interface with important consequences in the epitaxy associated with crystal nucleation processes.

## 2. Experimental

Stearic acid, octadecylamine, hexane, chloroform, strontium chloride and sodium carbonate were obtained from Aldrich chemicals and used without further purification.

A 50 ml solution of  $10^{-2}$  M stearic acid (SA) in chloroform was taken in a separating funnel and 50 ml of  $10^{-2}$  M aqueous solution of  $\text{SrCl}_2$  (pH = 6.2) was added. The biphasic mixture was allowed to rest for 1 h following which 15 ml of a  $10^{-2}$  M aqueous solution of  $\text{Na}_2\text{CO}_3$  was injected slowly into the aqueous side of the chloroform–water interface (solubility of  $\text{CHCl}_3$  in water is 0.08 w/w%; dielectric constant = 4.8; density = 1.47 g/ml). This leads to a super saturation ratio of ca. 350 in the salt solution. As the injection of  $\text{Na}_2\text{CO}_3$  progressed, the interface turned turbid and after some time it was noticed that crystals of  $\text{SrCO}_3$  were formed at the liquid–liquid interface. The organic solution was carefully removed from the separating funnel and the crystals formed at the interface were separated by filtration, washed with copious amounts of double distilled water and placed on Si (111) substrates for scanning electron microscopy (SEM) and X-ray diffraction (XRD) measurements. In a similar manner, the crystallization of  $\text{SrCO}_3$  was also carried out using octadecylamine (ODA) in chloroform as well as stearic acid in hexane, where  $\text{Na}_2\text{CO}_3$  was taken in aqueous phase (solubility of hexane in water is 0.001 w/w%; dielectric constant = 1.9; density = 0.66 g/ml).

In control experiments, the crystallization of  $\text{SrCO}_3$  was accomplished in a 50 ml chloroform/hexane (without stearic acid) – 50 ml  $\text{SrCl}_2$  biphasic mixture by injection of 15 ml of  $10^{-2}$  M aqueous solution of  $\text{Na}_2\text{CO}_3$ . The crystals were formed predominantly in the bulk of the aqueous solution and slowly settled down at the interface in the case of chloroform. Please note since the density of the chloroform is greater than that of water, the aqueous component rests on top of the organic solution and the crystals formed in the aqueous phase settle under the influence of gravity at the interface and at the bottom of

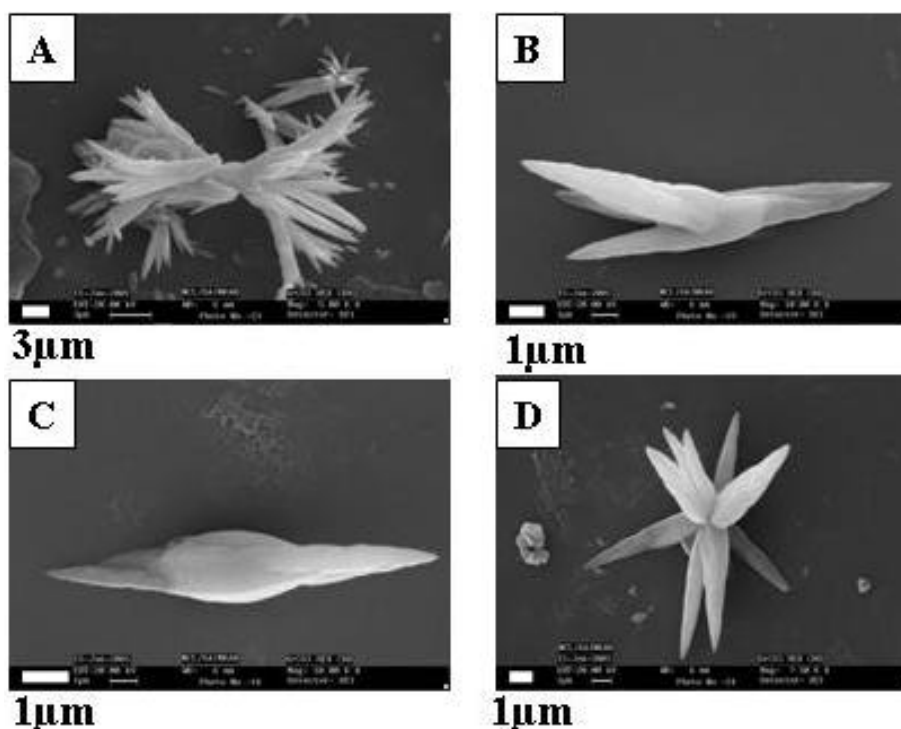
the reaction vessel in the case of hexane. The crystals grown in the bulk of the aqueous phase were studied by SEM. In order to understand the role of supersaturation on the morphology of  $\text{SrCO}_3$  crystals formed at the liquid–liquid interface, crystallization experiments were carried out with stearic acid in hexane at a supersaturation ratio of ca. 50 by adjusting the amount of  $\text{Na}_2\text{CO}_3$  solution ( $1.36 \times 10^{-3}$  M) injected into the aqueous component. In this experiment, crystal growth at the interface was extremely slow and the crystals were harvested for analysis after 12 h of reaction. In all the crystallization experiments, the temperature of the biphasic solutions was held at 25°C.

XRD analysis of all the  $\text{SrCO}_3$  samples deposited on Si (111) wafers was carried out on a Philips PW 1830 instrument operating in the transmission mode at 40 kV and a current of 30 mA with  $\text{CuK}_\alpha$  radiation. SEM measurements were carried out on a Leica Stereoscan-440 scanning electron microscope equipped with a Phoenix Energy Dispersive Analysis of X-rays (EDAX) attachment.

## 3. Results and discussion

The amphiphilic nature of the stearic acid molecules would lead to their adsorption at the liquid–liquid interface and enable electrostatic complexation of  $\text{Sr}^{2+}$  ions with the carboxylate groups of the fatty acid in a manner similar to that occurring at the air–water interface in the presence of anionic Langmuir monolayers (Heywood and Mann 1992a,b, 1994; Litvin *et al* 1997; Buijnsters *et al* 2001). It is well known that the concentration of these ions is 4–5 orders of magnitude larger than the concentration in the bulk of the aqueous solution leading to a high super saturation ratio at the interface. On similar lines, it would be expected that a similar metal ion concentration enhancement would occur at the hexane–water and chloroform–water interface in the presence of stearic acid molecules. Thereafter, reaction of the interface-bound  $\text{Sr}^{2+}$  ions with carbonate anions leads to the formation of  $\text{SrCO}_3$  at the liquid–liquid interface.

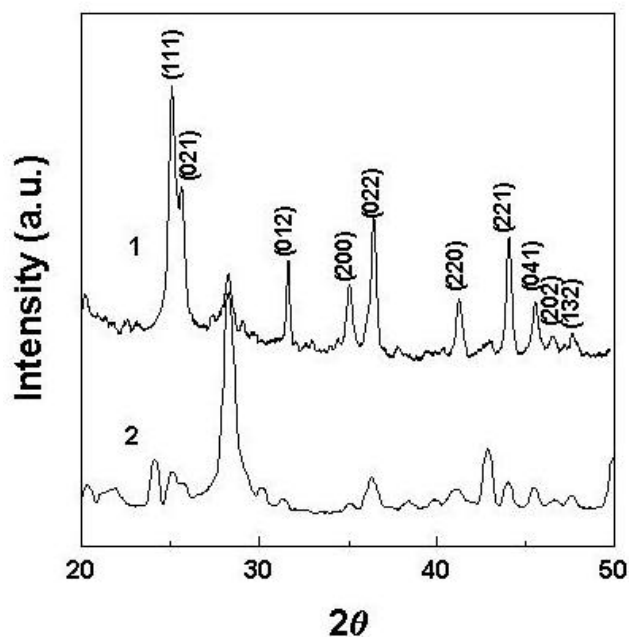
Figure 1 shows SEM images at different magnifications of  $\text{SrCO}_3$  crystallites grown at the water–chloroform interface with stearic acid as the additive at a SSR of 350. Sharp, strontianite needles are observed in all cases. Figure 1A also shows the branching of the strontianite needles at the tips (to the third level), a single branching of which is observed in figure 1B. Assembly of individual strontianite needles to yield a flower-like structure is seen in figure 1D and has been observed by us during the growth of  $\text{SrCO}_3$  crystals in lipid bilayer stacks (Sastry *et al* 2001). Spot profile EDAX measurements performed from within one part of the crystals which yielded a Sr : C : O ratio in excellent agreement with that expected for strontianite crystals. It can be seen that the crystals grow from the nucleation point and have



**Figure 1.** A–D. SEM micrographs at different magnifications recorded from  $\text{SrCO}_3$  crystals grown at the interface between water–chloroform interface with stearic acid molecules in the organic phase at 350 supersaturation ratio.

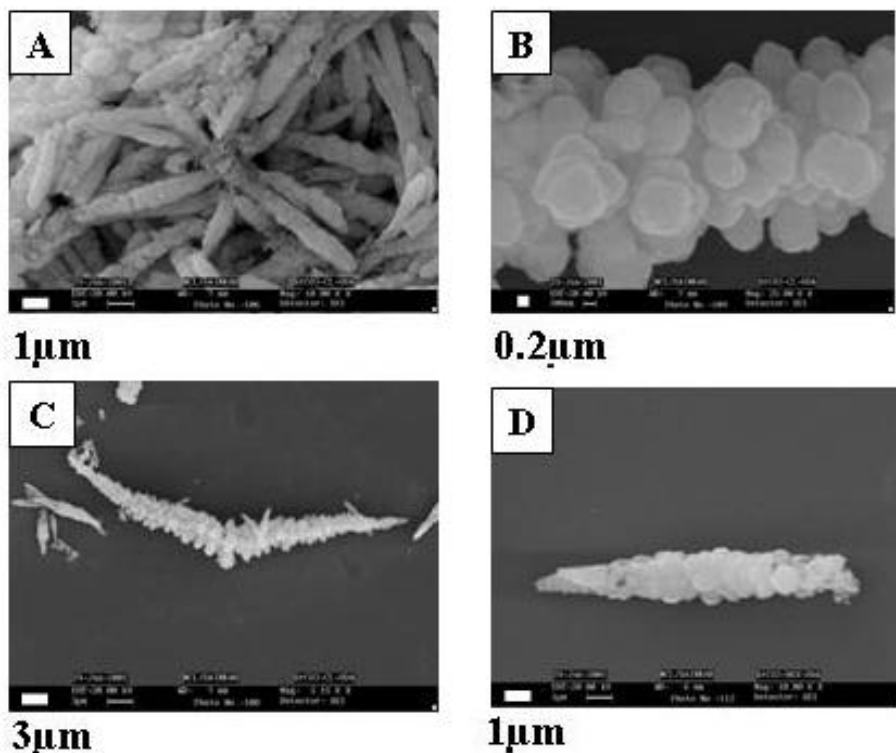
secondary branching at the tip of each crystallite. The XRD pattern recorded for this film is shown as curve 1 in figure 2. The Bragg reflections in the XRD pattern could be indexed with reference to the unit cell of the strontianite structure ( $a = 5.107 \text{ \AA}$ ,  $b = 8.414 \text{ \AA}$ ,  $c = 6.029 \text{ \AA}$ ; space group  $Pm\bar{c}n$ ) (ASTM chart).

Figure 3 shows SEM images recorded at different magnifications of  $\text{SrCO}_3$  crystals grown at the water–chloroform interface with octadecylamine as the templating molecule in the organic phase. In the case of ODA, the molecules at the interface would be positively charged at pH 6.2 and therefore, the carbonate ions would bind at the interface rather than  $\text{Sr}^{2+}$  ions, as was the case with stearic acid molecules. A comparison of figures 2 and 3 immediately reveals large and interesting differences in the morphology of the  $\text{SrCO}_3$  crystals grown in the two cases. The strontianite needles are much smaller in the case of crystals grown in the presence of ODA (figure 3A). Furthermore, on higher magnification it is observed that the individual needles possess strontianite crystals with spherical crystallites arranged around central needles (figure 3B). The needles grown near ODA monolayers appear to consist of aggregates of very uniform smaller crystallites (figures 3B–D). However, given the overall similarity in shape with strontianite needles grown in the presence of stearic acid (figure 1), it seems more likely that secondary nucleation around the core needle structures occurs leading to the interesting structure observed in the assembly. While the exact cause



**Figure 2.** XRD patterns recorded from  $\text{SrCO}_3$  crystals grown at the water–chloroform interface with stearic acid (curve 1) and octadecylamine in the organic phase (curve 2).

for this distinction in morphology of the strontianite crystallites in these two cases is not understood, given that the organic phase and supersaturation are identical in both experiments, the order in which the cation/anion is



**Figure 3.** A–D. SEM images of  $\text{SrCO}_3$  crystals grown at the interface between water and chloroform, the organic phase containing octadecylamine at 350 supersaturation ratio.

bound at the interface clearly plays a crucial role. This is an important aspect of this study and is in contrast to the results obtained by us on the growth of  $\text{BaSO}_4$  crystals at the liquid–liquid interface where the order of complexation of cation/anion at the interface was inconsequential (Ray *et al* 2001). We did not observe a significant difference in the morphology of  $\text{SrCO}_3$  crystals grown at the interface using hexane containing stearic acid/octadecylamine molecules (data not shown). The XRD pattern recorded from the crystals grown at the water–chloroform/hexane interface using octadecylamine and stearic acid are shown in figure 2 (curve 2). While the majority of the Bragg reflections could be indexed based on the strontianite structure, they are much reduced in intensity and broadened indicating very small crystallites.

In order to demonstrate that the differences in morphology of the strontianite crystals grown near stearic acid (figure 1) and octadecylamine (figure 3) monolayers are indeed due to the amphiphile, control experiments were performed wherein  $\text{SrCO}_3$  crystals were grown at an SSR of 350 in the water–chloroform biphasic solution without the amphiphile in the organic phase. Figure 4 shows SEM image of crystals grown under these conditions. It is seen that well-separated, flat strontianite needles are obtained in this case that are totally different from those shown in figures 1 and 3.

Another factor that could play a crucial role in determining the morphology of crystals grown at the liquid–



**Figure 4.** SEM image of  $\text{SrCO}_3$  crystals grown in a biphasic mixture of chloroform (without ionizable surfactant) and water in the control experiment.

liquid interface is the solution supersaturation. Figure 5 shows SEM images of  $\text{SrCO}_3$  crystals grown at the interface between water and chloroform containing stearic acid (figure 5A) and octadecylamine (figure 5B) at an SSR of 50. As in the case of the higher SSR experiments using stearic acid (figure 1), sharp strontianite needles with branching at the tips can be observed at a lower SSR

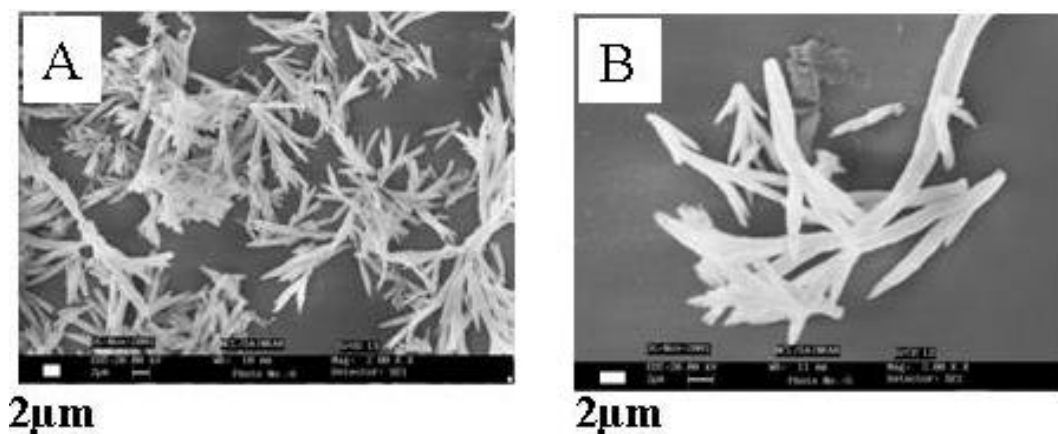


**Figure 5.** A–B. SEM images of  $\text{SrCO}_3$  crystals grown in a biphasic mixture of chloroform (with ionizable surfactant) and water at super saturation ratio ca.50.

as well (figure 5). However, at lower SSR values, the crystallites are smaller and thinner. In the case of fatty amine at the liquid–liquid interface, there are differences in the morphology of the crystals at high (figure 3) and low SSRs (figure 5B). The well-defined structure in the strontianite needles is not observed at lower SSRs and indicates that their formation could be determined by kinetic effects. However, the fact that the morphology of strontianite needles at lower SSRs is also influenced by the additive at the interface is clearly borne out by a comparison of the SEM images in figures 5A and B. The sensitivity of the morphology of strontianite crystals to the nature of the surfactant (cationic or anionic) as well as the super saturation ratio is a salient feature of this study. Figure 6 shows XRD patterns recorded from the  $\text{SrCO}_3$  crystals grown at SSR 50 in the presence of stearic acid (curve 1) and octadecylamine (curve 2). As in the previous experiments, the Bragg reflections are characteristic of strontianite and have been indexed accordingly.

The morphology of the strontianite crystals of this study grown in the presence of cationic or anionic surfactants is completely different from that of  $\text{SrCO}_3$  crystals grown in thermally evaporated lipid films (Sastry *et al* 2001) and self-assembled monolayers of alkanethiols on gold surfaces (Kunther *et al* 1998a). It appears that the fatty acid/fatty amine molecules at the liquid–liquid interface behave in a manner similar to crystal growth inhibitors. This may be a consequence of the finite solubility of the two solutions leading to a fairly broad interfacial region where the fatty lipid molecules are relatively evenly distributed. This would enable the lipid molecules to bind to nascent crystals growing at the interface and thereby, control the growth of specific crystallographic faces and the crystal morphology. We believe that the electrostatic interaction between the  $\text{Sr}^{2+}$  ions and the fatty acid molecules would also be modulated by the lower dielectric

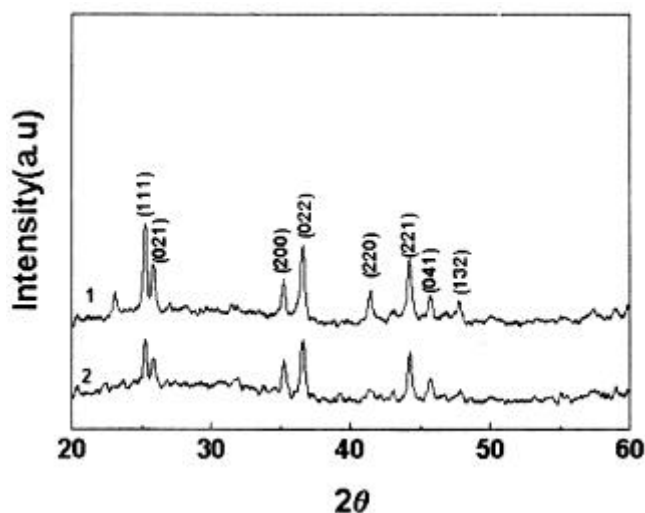


**Figure 6.** XRD patterns recorded from  $\text{SrCO}_3$  crystals grown at the water–chloroform interface with stearic acid (curve 1) and octadecylamine (curve 2) in the organic phase at super saturation ratio 50.

constant of the organic component within the interfacial region. It is also possible that the polarity changes at the interface could affect the orientation and solvation of alkyl chains in the organic phase, which could control the growth of crystallites (Ishizaka *et al* 2001). The splitting of crystals over generations and the number of splits and opening angles in each generation could be due to intrinsic field effects at the nucleating centres (Busch *et al* 1999; Kniep and Busch 1996). While the exact details of the mechanism for morphology variation of strontianite crystals at the liquid–liquid interface need to be worked out, it is clear that the use of such interfaces provides exciting possibilities for tailoring the growth mode of crystals.

#### 4. Conclusion

It has been shown that strontianite crystals may be grown at the liquid–liquid interface with suitable surfactants and at different super saturation ratios to control the morphology of the crystals at the interface. The use of the liquid–liquid interface throws open the exciting possibility of tailoring the physical and chemical properties of the interface and thereby, modifying the morphology of the crystals nucleating and growing at the interfaces.

#### Acknowledgements

(SR) and (DR) are thankful to the University Grants Commission and the Department of Science and Technology, Govt. of India, for financial assistance. Useful discussion with Mr Ashavani Kumar is gratefully acknowledged.

#### References

- Addadi L and Weiner S 1992 *Angew. Chem. Int. Ed. Engl.* **31** 153
- Aizenberg J, Black A J and Whitesides G M 1999 *J. Am. Chem. Soc.* **121** 4500
- Bowen N, Arias F, Deng T and Whitesides G M 2001 *Langmuir* **17** 1757
- Bowers J, Aarbaksh A, Webster J R P, Hutchings L R and Randall R W 2001 *Langmuir* **17** 140
- Bromley L A, Cottier D, Davey R J, Dobbs B, Smith S and Heywood B R 1993 *Langmuir* **9** 3594
- Buijnsters P J J A, Donners J J J M, Hill S J, Heywood B R, Nolte R J M, Zwanenburg B and Sommerdijk N A J M 2001 *Langmuir* **17** 3623
- Bunker B C *et al* 1994 *Science* **264** 48
- Busch S *et al* 1999 *Eur. J. Inorg. Chem.* 1643
- Falini G, Gazzano M and Ripamonti A 1994 *Adv. Mater.* **6** 46
- Feng S and Bein T 1994 *Science* **265** 1839
- Heuer A H *et al* 1992 *Science* **255** 1098
- Heywood B R and Mann S 1992a *Langmuir* **8** 1492
- Heywood B R and Mann S 1992b *J. Am. Chem. Soc.* **114** 4681
- Heywood B R and Mann S 1994 *Adv. Mater.* **6** 9 and references therein
- Hopwood J D and Mann S 1997 *Chem. Mater.* **9** 950
- Ishizaka S, Kim H B and Kitamura N 2001 *Anal. Chem.* **73** 2421
- Kniep R and Busch S 1996 *Angew. Chem. Int. Ed.* **35** 2624
- Kuther J, Nelles G, Seshadri R, Schaub M, Butt H-J and Tremel W 1998a *Chem. Eur. J.* **4** 1834
- Kuther J, Seshadri R, Nelles G, Butt H J, Knoll W and Tremel W 1998b *Adv. Mater.* **10** 401
- Kuther J, Seshadri R and Tremel W 1998c *Angew. Chem. Int. Ed.* **37** 3044
- Kuther J, Seshadri R, Nelles G, Assenmacher W, Butt H-J, Mader W and Tremel W 1999 *Chem. Mater.* **11** 1317
- Litvin A L, Valiyaveetil S, Kaplan D L and Mann S 1997 *Adv. Mater.* **9** 124
- Li M and Mann S 2000 *Langmuir* **16** 7088
- Mann S 1993 *J. Chem. Soc. Dalton Trans.* 1
- Mann S 1996 *Inorganic materials* (eds) D W Bruce and D O'Hare (John Wiley & Sons) p. 255
- Mann S 1997 *J. Chem. Soc. Dalton Trans.* 3953
- Mann S, Webb J and Williams R J P 1989 *Biomaterialization, chemical and biochemical perspectives* (Wiley-VCH, Weinheim)
- McGrath K M 2001 *Adv. Mater.* **13** 989
- Nagtegaal M, Seshadri R and Tremel W 1998 *Chem. Commun.* 2139
- Qi L, Coffen H and Antonietti M 2000 *Angew. Chem. Int. Ed.* **39** 604
- Ray D R, Kumar A, Reddy S, Sainkar S R, Pavaskar N R and Sastry M 2001 *CrystEngComm.* 45
- Sastry M, Kumar A, Damle C, Bhagwat M and Ramaswamy V 2001 *CrystEngComm.* 19
- Sathaye S D, Patil K R, Paranjape D V, Mitra A, Awate S V and Mandale A B 2000 *Langmuir* **16** 3487
- Uchida M, Sue A, Yoshioka T and Okuwaki A 2001 *CrystEngComm.* 5
- Weiner S and Addadi L 1997 *J. Mater. Chem.* **7** 689